

## ZnO hexagonal arrays of nanowires grown on nanorods

R. C. Wang, C. P. Liu,<sup>a)</sup> and J. L. Huang  
*Department of Materials Science and Engineering, National Cheng Kung University,  
 Tainan 70101, Taiwan*

S.-J. Chen  
*Department of Chemical and Material Engineering, National Kaohsiung University of Applied Sciences,  
 Kaohsiung 80778, Taiwan*

(Received 17 February 2005; accepted 11 May 2005; published online 15 June 2005)

ZnO single-crystalline nanowire-type nanostructures were synthesized on silicon by thermal chemical vapor deposition without catalysts through a two-step pressure-controlled vapor-reflected process at a low temperature of 550 °C where self-organized hexagonal crystalline or porous nanowire arrays were grown on nanorods. The nanowire diameter is around 20 nm and number of nanowires is selected by the nanorod size. Cathodoluminescence spectra exhibit strong green emissions, indicative of high oxygen-vacancy density, which sheds a light on further applications for multichannel nanoconductors in nanodevices. © 2005 American Institute of Physics. [DOI: 10.1063/1.1948522]

ZnO one-dimensional (1D) nanostructures for nano-optoelectronic devices such as UV lasing<sup>1</sup> have received special attention because of the characteristics of a direct wide band gap of 3.37 eV and large exciton binding energy of 60 meV at room temperature. ZnO 1D nanostructures have also attracted notice as possibly ideal nanoconductors in optoelectronics due to both high thermal stability and electrical conductivity for intrinsic oxygen vacancy. Therefore, for this application, a vapor trapping chemical vapor deposition method was developed to obtain high conductive ZnO nanowires with a high density of oxygen vacancies.<sup>2</sup>

The potential application rests upon the shape of 1D nanostructures. However, the previously reported 1D nanostructures such as nanowires, nanorods, nanoneedles, nanobelts, and nanoribbons all have a monotonic line shape with a port at one end, which restricts them from being applied in advanced systems. However, multifunctional devices capable of communicating with many receivers would require higher integrated nanostructures with many channels.

In this letter, we report on the fabrication of ZnO nanowire-type nanostructures where well organized hexagonal arrays of nanowires were grown on nanorods by a two-step pressure-controlled vapor-reflected thermal evaporation method at a low temperature of 550 °C. Cathodoluminescence spectra of both the nanowires and nanorods of the nanowire-type nanostructures exhibit strong green emissions, which indicate that the nanowire-type nanostructures possess high electrical conductivity and are promising candidates for electron nanoconductors in multichannel optoelectronic devices.

The ZnO nanowire-type nanostructures were synthesized via a two-step pressure-controlled vapor-reflected thermal evaporation deposition. A silicon (100) wafer and zinc powders (purity: 99.8%) were inserted into a horizontal quartz tube and a 1 mm gap was set between the sources and the substrate. As distinct from the conventional method of thermal evaporation, neither tedious catalysts nor additives were

needed. Notably, a 3 mm high glass plate acting as a reflecting wall was placed on the Si substrate 8 mm away from the source to achieve a vapor-reflected effect. During the experiment, the sources were heated at a rate of 20 °C/min from room temperature. Argon at a flow rate of 54 sccm was introduced into the deposition system. Once the temperature was raised to 450 °C, oxygen was switched on at a flow rate of 3 sccm. The working pressure was kept at 15 Torr. After heating at 550 °C for 30 min, the substrate was slowly cooled down in the furnace and the working pressure was decreased from 15 to 5 Torr.

The morphology of the prepared film was examined with field-emission scanning electron microscopy (SEM). As shown in Fig. 1(a), nanowire-type nanostructures comprised of well organized nanowire arrays connected with hexagonal faceted nanorods were grown on the substrate. The nanorods have an average diameter of 400 nm while the nanowires are in a range of 15–25 nm in diameter. An enlarged view and a schematic diagram of the embryos of the nanowires are shown in Figs. 1(b) and 1(c), respectively, exhibiting the hexagonal array characteristics. The spacing between individual nanowires is around 60 nm. The nanoscale spatial pattern could be attributed to the adsorption-desorption kinetics and nonlinear diffusion of atoms in a deposited layer

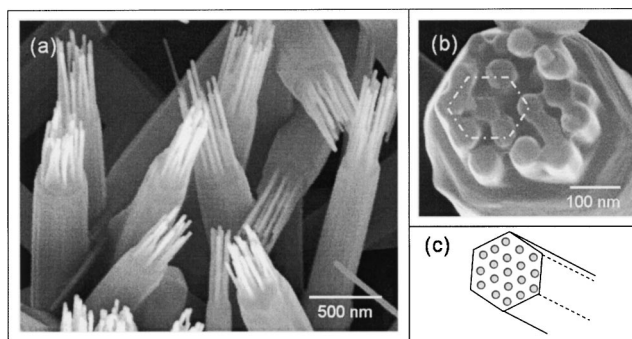


FIG. 1. (a) High-magnification SEM image of nanowire-type nanostructures. (b) An enlarged view of the embryos of the nanowires, exhibiting the hexagonal array characteristic. (c) Schematic diagram of the hexagonal nanowire array.

<sup>a)</sup> Author to whom correspondence should be addressed; also at: Center for Micro/nano Technology Research, National Cheng Kung University, Tainan 70101, Taiwan; electronic mail: cpliu@mail.ncku.edu.tw

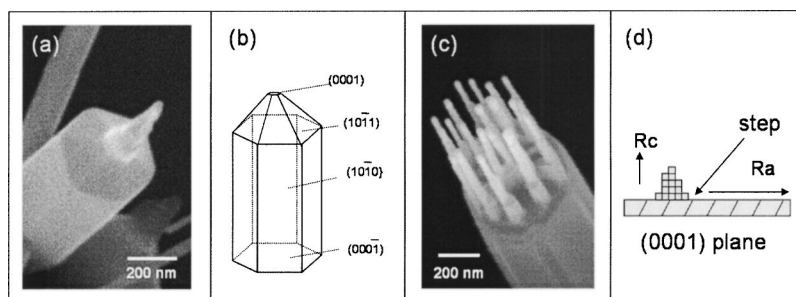


FIG. 2. (a) SEM image of a nanopencil grown by a two-step pressure-controlled thermal evaporation without a reflecting wall. (b) The schematic idealized growth habit of ZnO. (c) SEM image of a nanowire-type nanostructure grown with a reflecting wall assisted two-step pressure-controlled thermal evaporation. (d) Schematic diagram of steps formation leading to hillocks grown on the (0001) face of ZnO.

at relative low temperature and sufficiently high atomic mobility.<sup>3</sup> Beyond this, on carefully examining the nanostructures, the nanowires were found to be self-organized in several distinct hexagonal arrays. Furthermore, the number of the nanowires on a nanorod is approximately proportional to the area of the top (0001) platform of a nanorod, indicating the constant nanowire density.

Here we propose a growth mechanism for the morphology of the nanowire-type nanostructures, where the growth could be separated into two stages. The first stage is the growth of the nanorods along the [0001] direction. Because no catalysts are used, the growth is different from the traditional vapor-liquid-solid mechanism. The nanorods apparently nucleated via a self-catalyzed mechanism.<sup>4</sup> Laudise and Ballman claimed that the formation of the hexagonal prismatic shape of ZnO rod-like crystals can be attributed to the different growth rates of various growth facets,<sup>5</sup> following in the order of  $[0001] > [10\bar{1}1] > [10\bar{1}0]$ . Accordingly, while the surface diffusion process is the most important rate-limiting step in the ZnO crystal growth, the (0001) plane easily disappears and instead is bounded by higher Miller indices but with a lower specific surface energy such as (10 $\bar{1}$ 1) plane to form a common tip shape. However, in the designed vapor-reflected growth process demonstrated in this letter, the increased convection may enhance the surface diffusion in a lateral direction (a) with respect to the vertical direction (c) so as to accelerate the movement of steps relative to the nucleation of new steps.<sup>6</sup> Therefore, the (0001) planes are the most likely facets which remain without (10 $\bar{1}$ 1) after the growth.

The second stage is the growth of the nanowires on the nanorods, when the working pressure was decreased suddenly at the beginning of the slow cooling process, which should correspond to the termination of the nanorod growth due to the shortage of the source vapor. In the first growth process, though the top (0001) surface is macroscopically flat, nanoscale roughness may be still formed due to adsorption-desorption kinetics and nonlinear diffusion of atoms.<sup>3</sup> In the second growth stage during cooling, the lower pressure of both evaporated zinc and oxygen flux would favor the nucleation of the finer nanowires from those previously formed high coverage spots of the nanoscale spatial pattern.

To support the proposed mechanism, we compare the resulting nanostructure morphology from the growth experiment with and without the reflecting wall while maintaining other growth conditions as before in Fig. 2. Without the reflecting wall, nanorods exhibit typical nanopencil morphology with a sharp tip bounded by (10 $\bar{1}$ 1) in the first growth stage [Figs. 2(a) and 2(b)], followed by a single tapered nanowire grown on the tip in the second growth stage. In

contrast, Figs. 2(c) and 2(d) show the SEM image of a nanowire-type nanostructure grown by a reflecting wall assisted two-step pressure-controlled thermal evaporation and the schematic diagram of steps formation leading to hillocks grown on the (0001) face of ZnO,<sup>6</sup> respectively.

The detailed microstructures of the ZnO nanowire-type nanostructures were studied using a JEOL 2100F field emission transmission electron microscope (TEM). Figure 3(a) shows a typical low-magnification TEM image of the nanostructure. The nanowires are parallel to each other indicating good configuration for nanoconductors applications. High-resolution TEM observations and electron diffraction, shown in Figs. 3(b) and 3(c), show that both the nanorods and nanowires are single-crystalline structures growing along the [0001] direction. Furthermore, few nanowire-type nanostructures composed of porous nanowires were also found. Figures 3(d) and 3(e) are the low and medium-magnification TEM images of the porous nanowires of a nanowire-type nanostructure. Figures 3(f) and 3(g) show the high-resolution image and electron diffraction pattern of these porous nanowires, respectively, which indicate that these porous nanowires are also single-crystalline structures growing along the [0001] direction. These porous nanowires may have more interesting optoelectronic properties due to quantum confinement.

Figure 4 shows the room temperature cathodoluminescence (CL) spectra of both the nanowires and nanorods of

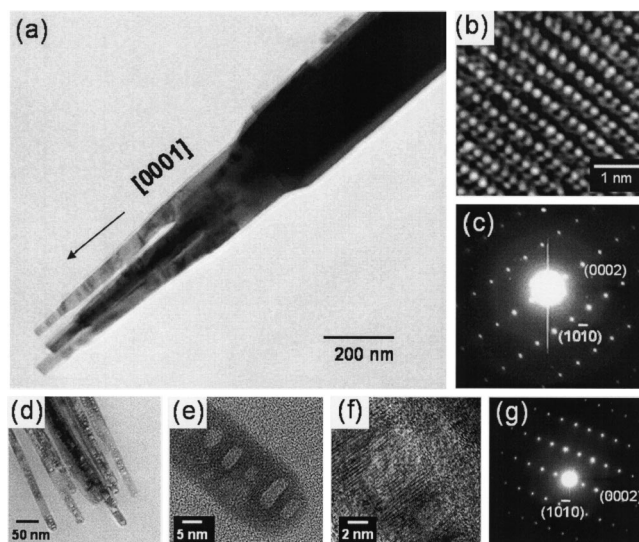


FIG. 3. (a) A typical low-magnification TEM image of a nanowire-type nanostructure. (b) High-resolution TEM observation of the nanowires. (c) Electron diffraction of the nanowire-type nanostructure. (d)–(e) low and medium-magnification TEM image of a nanowire-type nanostructure with porous nanowires. (f) High-resolution TEM image of the porous nanowires. (g) Electron diffraction of the porous nanowires.

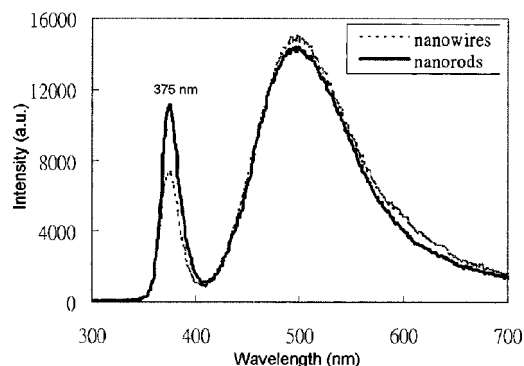


FIG. 4. Room temperature CL spectra of both the nanowires and nanorods of the nanowire-type nanostructures.

the nanowire-type nanostructures. Both spectra exhibit relatively sharp UV emission centered at around 375 nm and strong green emission centered at around 500 nm. The UV emission is attributed to the free exciton recombination at the near-band edge, while the green emission may be a result of the transition between the photoexcited holes and singly ionized oxygen vacancies.<sup>7</sup> The nanowires with high density of oxygen vacancies have been shown to have a higher electrical conductivity than those with only few oxygen vacancies,<sup>2</sup> indicating that the nanowire-type nanostructures are promising candidates as electron nanoconductors in nano-optoelectronic devices. Furthermore, it was reported that the oxygen vacancies responsible for the green emission are located at the surface.<sup>8</sup> Therefore, the ratio of UV to green emission is dependent on the nanostructure's size.<sup>9</sup> Consequently, the fact that the nanowires have a higher ratio of green to UV emission than nanorods may result from their relatively larger surface areas.

In summary, the ZnO single-crystalline nanowire-type nanostructures were synthesized via a simple two-step pressure controlled vapor-reflected thermal evaporation without catalysts at a low temperature of 550 °C. The nanostructures possess hexagonal arrays of nanowires grown on top of nanorods along the [0001] direction. CL spectra from the nanostructures exhibit strong green emission, indicative of high oxygen-vacancy density. This implies that the nanowire-type nanostructures are promising candidates as electron nanoconductors in nano-optoelectronic devices.

The work was supported by Research Grant No. NSC93-2120-M-006-007, National Science Council of Taiwan. The authors are grateful to Professor K. H. Chen, Professor L. C. Chen, and C. W. Hsu for the CL experiments and helpful discussions. The authors thank the Center for Micro/nano Technology Research, National Cheng Kung University, Taiwan for the provision of the HRTEM.

<sup>1</sup>M. H. Huang, S. Mao, H. Feick, H. Q. Yan, Y. Wu, H. Kind, E. Weber, R. Eusso, and P. Yang, *Science* **292**, 1897 (2001).

<sup>2</sup>P. C. Chang, Z. Fan, D. Wang, W. Y. Tseng, W. A. Chiou, J. Hong, and J. G. Liu, *Chem. Mater.* **16**, 5133 (2004).

<sup>3</sup>D. Walgraef, *Physica E (Amsterdam)* **15**, 33 (2002).

<sup>4</sup>J. Q. Hu, Q. Li, N. B. Wong, C. S. Lee, and S. T. Lee, *Chem. Mater.* **14**, 1216 (2002).

<sup>5</sup>R. A. Laudise and A. A. Ballman, *J. Phys. Chem.* **64**, 688 (1960).

<sup>6</sup>R. A. Laudise, E. D. Kolb, and A. J. Caporaso, *J. Am. Ceram. Soc.* **47**, 9 (1964).

<sup>7</sup>K. Vanhausden, W. L. Warren, C. H. Seager, D. R. Tallant, J. A. Voigt, and B. E. Gnade, *J. Appl. Phys.* **79**, 7983 (1996).

<sup>8</sup>D. Li, Y. H. Leung, A. B. Djuricic, Z. T. Liu, M. H. Xei, S. L. Shi, S. J. Xu, and W. K. Chan, *Appl. Phys. Lett.* **85**, 1601 (2004).

<sup>9</sup>M. H. Huang, Y. Wu, H. Feick, N. Tran, E. Weber, and P. Yang, *Adv. Mater. (Weinheim, Ger.)* **13**, 113 (2001).